scientific reports

Check for updates

OPEN

Secondary products and molecular mechanism of calcium oxalate degradation by the strain *Azospirillum* sp. OX-1

Dening Xia[1], Wenjun Nie[1], Xiaofang Li[1], Roger D. Finlay[2] & Bin Lian[1]✉

The oxalate-carbonate pathway (OCP) involves degradation of soil oxalate to carbonate. To exploit and manage this natural mineralization of assimilated atmospheric CO_2 into stable carbonates, improved understanding of this complex biotransformation process is needed. A strain of oxalate-degrading bacteria, *Azospirillum* sp. OX-1, was isolated from soil, and its secondary products of calcium oxalate degradation were analyzed and characterized using SEM, XRD, TG/DTG-DTA and FTIR-spectroscopy. The molecular mechanism of calcium oxalate degradation was also analyzed using proteomics. The results showed, for the first time, that OX-1 could not only degrade calcium oxalate to calcium carbonate, but also that the process was accompanied by synthesis of methane. Proteomic analysis demonstrated that OX-1 has a dual enzyme system for calcium oxalate degradation, using formyl-CoA transferase (FRC) and thiamine pyrophosphate (ThDP)-dependent oxalyl-CoA decarboxylase (OXC) to form calcium carbonate. Up-regulated expression of enzymes related to methane synthesis was also detected during calcium oxalate degradation. Since methane is also a potent greenhouse gas, these new results suggest that the utility of exploiting the OCP to reduce atmospheric CO_2 must be re-evaluated and that further studies should be conducted to reveal how widespread the methane producing capacity of strain OX-1 is in other bacteria and soil environments.

Keywords Oxalate-degrading bacteria, Carbonate, Methane, OCP, Proteome, Molecular mechanism

It is well known that during biological weathering of soil minerals, some plants and many fungi release organic acids, among which oxalic acid plays an important role[1–4]. However, oxalic acid easily combines with some metal ions (e.g. calcium and magnesium) to form insoluble, crystalline oxalate minerals (e.g. calcium oxalate ($Ksp = 4.0 \times 10^{-8}$) and magnesium oxalate ($Ksp = 8.57 \times 10^{-5}$)), which can also assume various shapes (prismatic, needle-like, nucleated) and varying degrees of hydration (e.g. calcium oxalate monohydrate, magnesium oxalate dihydrate)[5]. These crystals cover the surface of root hairs and mycelia, thus affecting the continuous utilization of mineral nutrients by plants and soil organisms. Fortunately, oxalates can be broken down by oxalate-degrading bacteria even some special fungi in soil and converted into carbonates (such as calcium oxalate crystal into calcite), thus reducing the adverse effects of oxalate crystals on plant growth[6]. Oxalic acid and oxalate are found in a variety of ecosystems, in both terrestrial and aquatic environments[7,8] and in the gastrointestinal tract of mammals[9].Despite the diversity of ecological niches of oxalic acid and oxalate, the lack of evidence of calcium oxalate accumulation in geological sediments[10] suggests the presence of multiple taxa in the soil that can degrade oxalate.

Although some wood-rotting fungi can also degrade oxalate[11], most soil oxalate is decomposed and utilized by bacteria, which are usually called oxalotrophic[12]. Such bacteria have been isolated from tropical forest soils[13,14], temperate forest soils[15] and urban soils[16]. Oxalate-degrading bacteria include specialized oxalate-degrading bacteria capable of using oxalate as the sole source of carbon and energy. For example, *Oxalobacter formigenes* is a unique anaerobic bacterium and was the first oxalate-degrading bacterium to be isolated, relying only on oxalate for growth[17]. Degradation of oxalate in the gut by this bacterium plays a key role in the prevention of nephrotoxicity in animals feeding on oxalate-rich plants[18]. Many more oxalate-degrading bacteria are facultative, and can use oxalates as a carbon source, as well as other substrates, including some species of *Bacillus*, *Burkholderia*, *Streptomyces*, *Alkaligenes* and *Lactobacillus*[10,19–21].

[1]College of Life Sciences, College of Marine Science and Engineering, Nanjing Normal University, Nanjing 210023, China. [2]Department of Forest Mycology and Plant Pathology, Uppsala BioCenter, Swedish University of Agricultural Sciences, Uppsala 75007, Sweden. ✉email: bin2368@vip.163.com

There are three main pathways for the degradation or oxidation of oxalate in the environment. Oxalate oxidase found mainly in higher plants, catalyzes the degradation of oxalate to CO_2 and H_2O_2, and its main function is to promote seed germination and defend against pathogenic bacteria[22,23]. The second pathway involves oxalate decarboxylase mainly present in fungi and some bacteria, which catalyzes the degradation of oxalate to formic acid and CO_2, requiring the presence of oxygen. The third pathway involves formyl-CoA transferase (FRC) and thiamin pyrophosphate-dependent oxalyl-CoA decarboxylase (OXC), which are mainly distributed in bacteria, the dual enzyme system consisting of these two enzymes undertakes the main degradation process of soil oxalate[24]. FRC (EC 2.8.3.16) and OXC (EC 4.1.1.8) are encoded by the *frc* and *oxc* genes, respectively, and the *frc* gene has been used as an indicator to study the molecular diversity and abundance of oxalate-degrading bacteria[25]. Sun, et al.[26] used the *frc* gene to identify the diversity and community structure of ectomycorrhizal fungal rhizosphere oxalate-degrading bacteria. When oxalate-degrading bacteria degrade oxalate, metal ions immobilized by oxalate are re-solubilised, thus significantly improving the efficiency of metal ion (calcium, magnesium, etc.) utilization by plants and soil microorganisms[27] and facilitating biogeochemical cycling of metal elements[28].

The process of assimilation of CO_2 by green plants or photosynthetic microorganisms to produce organic carbon through photosynthesis is well known, but the carbon sink role and environmental significance of the conversion of large amounts of oxalate to carbonate formed by plant roots have been underestimated or even ignored. The metabolic pathway from oxalate to carbonate, the oxalate carbonate pathway (OCP), involves the synergistic action of plants, saprophytic decomposers and oxalate-degrading bacteria to both promote the use of soil organic carbon and improve soil rhizosphere ecology, and to increase soil carbonate content[29–32]. Since carbonates are usually stable for 10^2-10^6 years, the widespread oxalate-carbonate conversion process has an important impact on the regulation of atmospheric CO_2 concentration[33,34]. The researchers focused on the solid metabolites generated by bacteria degradation of oxalate in the past, and ignored the gas generated by the metabolism and the transformation. To effectively utilize this process of carbon capture, and promote the transformation of photosynthetic carbon into a stable form in the soil, it is necessary to perform an in-depth study of the molecular mechanism used by oxalate-degrading bacteria, and to investigate the main secondary products and their physiological functions in the oxalate degradation process. This will improve our understanding and exploitation of natural carbon capture, assimilation and biomineralization processes.

In the present study, an efficient strain of oxalate-degrading bacteria was isolated from soil, and the carbon-containing secondary products in the OCP pathway were analyzed using SEM, XRD, FTIR, TG/DTG-DTA and GC. Proteomics was used to analyze the mechanism of calcium oxalate degradation by this strain and secondary product formation at the molecular level, and to improve the understanding of the ecological function of the OCP pathway.

Materials and methods

Isolation and 16S rRNA gene sequence analysis of oxalate-degrading bacteria

The target strains were isolated from soil samples taken at Nanjing Normal University, Xianlin Campus Botanical Garden (32°06′N, 118°54′E) using enrichment culture followed by dilution coating plate isolation[35]. Single colonies that grew well on calcium oxalate solid medium were selected and incubated on LB solid medium (Tryptone 1%; NaCl 1%; Yeast extract 0.5%; Agar 1.5%) for further purification. The isolated strains were inoculated back into calcium oxalate liquid medium (Calcium oxalate 1%; Yeast extract 0.05%; K_2HPO_4 0.005%; $MgSO_4{\cdot}7H_2O$ 0.005%; pH 7.0) and incubated for 48 h at 30 °C and 180 rpm in a shaker (ZQZY-C8E, Shanghai Zhichu Instrument Co., Ltd.). The precipitate was collected by centrifugation at 9000 rpm for 10 min, dried at 65 °C and then subjected to X-ray diffraction (BTX-526, Olympus, USA) to determine its mineral composition and to observe whether calcium oxalate was degraded and whether new minerals (carbonates) were formed. Using this method, we found strain OX-1 with high efficiency in the degradation of calcium oxalate for use in the follow-up study.

The 16S rRNA gene of the isolated strain OX-1 was sequenced using the universal primer 27F/1492R, and the obtained 16S rRNA sequences were compared with those in the NCBI database. MEGA 6.0 software was used to perform multiple sequence alignment analysis and construct a phylogenetic tree using the neighbor-joining method.

Morphology and growth characteristics of strain OX-1

The OX-1 was inoculated onto LB solid medium at 30 °C for 48 h in an inverted position. And the colony color, morphology and growth were observed and recorded. OX-1 was cultured in LB liquid medium to the exponential growth phase ($OD_{600} \approx 0.5$–0.8), centrifuged at 3000 rpm for 10 min to collect the bacterial precipitate, and washed 1–2 times with PBS. The supernatant was discarded and pre-cooled fixative (2.5% glutaraldehyde) at 4 °C was slowly added along the wall of the tube, before refrigeration at 4 °C overnight prior to subsequent processing. The treated organisms were observed by scanning electron microscopy (HITACHI SU8100, Japan) to examine microscopic morphology.

Two wire inoculation loops of strain OX-1 were added to 100 mL LB liquid medium, shaking at 30 °C, 180 rpm for 48 h. The growth curve of OX-1 was drawn by measuring OD_{600} of culture medium every 4 h. According to *Berger's Manual of Bacterial Identification* (Ninth edition)[36], nitrogen fixation, cellulase, amylase, gelatin liquefaction, peroxidase, methyl red (M-R), voges-proskauer (V-P), urease, nitrate reduction and hydrogen sulfide production were tested to understand the physiological and biochemical properties of OX-1.

Biodegradation of calcium oxalate by strain OX-1 and analysis of secondary minerals

To investigate the degradation characteristics of oxalate by strain OX-1, calcium oxalate was chosen as the main carbon source. Bacteria were cultured in 100 mL of sterile calcium oxalate liquid medium in 250-mL conical flasks with an uninoculated control and incubated in a constant temperature shaker at 30 °C and 180 rpm for 7 d. The pH, $C_2O_4^{2-}$and Ca^{2+} concentrations of the culture solution were measured at 24 h intervals, and precipitates collected by centrifugation were analyzed. The oxalate content of the samples was determined using a colorimetric method[35]. The samples were centrifuged at 6000 rpm for 10 min, pH was adjusted to 2 with 6 M HCl, and the supernatant was analyzed using the colorimetric method. Measurements were carried out using a microplate reader SpectraMax M2 (Molecular Devices, USA) at 660 nm. The concentrations of Ca^{2+} in the supernatant was determined with atomic absorption spectrometry (AAS, AA-6300 C, Shimadzu, Japan). The morphology, elemental composition, crystal structure, organic functional group distribution and thermal stability of the secondary minerals formed during the degradation of calcium oxalate were characterized analysis using X-ray diffraction (XRD, BTX-526, Olympus, USA), Fourier transform infrared spectrometry (FTIR, Bruker, Hyperion 2000, DEU), simultaneous thermal analysis (TGA-DTA, PerkinElmer, Diamond DMA, USA) (test conditions: from 25 °C to 1000 °C at 10 °C/min under an N_2 atmosphere), scanning electron microscopy and energy spectrum analysis (SEM-EDS, Zeiss Supra 55-Oxford Aztec X-Max 150).

Determination of methane content during the biodegradation of calcium oxalate by strain OX-1

Bacteria were inoculated in 250-mL conical flasks with 100 mL calcium oxalate liquid medium, as before, and incubated shaking at 30 °C and 180 rpm. 8 layers of absorbent gauze and 4 layers newspaper were used to seal the opening of the conical flask. The headspace gas in the culture flasks was collected with a 10 mL syringe after 36 h incubation. The concentration of methane produced during the experiment was determined using gas chromatography (GC, Agilent Technologies 7890B). Chromatographic column: HayeSep $N+5$ A (2.44 m×2 mm), HayeSep Q (0.9 m×2 mm). Carrier gas: high purity nitrogen (99.999%), carrier gas flow rate 2 mL/min, the inlet temperature was 150 °C and the column temperature was maintained at 80 °C for 18 min. The FID pre-detector temperature was 200 °C, and TCD post-detector temperature 150 °C.

4D-label-free proteomic analysis and verification

Strain OX-1 was grown in a calcium oxalate environment, in which calcium oxalate was the main carbon source (C group), as well as a calcium oxalate-free environment where the main carbon source was glucose (G group as CK). Three biological replicates were incubated at 30 °C with shaking at 180 rpm. After 36 h incubation samples were taken from the culture medium and centrifuged at 4 °C, 9000 rpm for 10 min. The supernatant was discarded and residual precipitate washed with PBS buffer 2–3 times and recentrifuged under the same conditions; The final sample were frozen in liquid nitrogen and stored at -80 °C prior to 4D-label-free proteomic analysis.

The differentially expressed proteins were screened according to the following standards: Foldchange ≥ 2.0 or Foldchange $\leq 1/2.0$ and P-value < 0.05. The mass spectrometry proteomics data have been deposited at the Proteome Xchange Consortium (http://proteomecentral.proteomexchange.org) via the iProX partner repository with the dataset identifier PXD041599. After identifying differentially expressed proteins (DEPs), we extracted each annotation information based on Uniprot, KEGG, GO, KOG/COG and other databases to explore protein functions. GO/KEGG enrichment analysis was performed on these proteins to characterize their functions.

To further verify the 4D-label-free proteomics results, we selected proteins related to oxalate degradation, methane synthesis, and antioxidant mechanisms for Parallel Reaction Monitoring (PRM) validation of key differential proteins.

Results

Identification and characteristics of strain OX-1 and its oxalate degradation ability

Identification and growth characteristics of strain OX-1

Multiple strains of calcium oxalate-degrading bacteria were obtained by screening in a liquid medium with calcium oxalate as the main carbon source. The strain designated OX-1 had the highest degradation efficiency.

After cultured in LB solid medium for 5 days, the OX-1colonies were round, about 10 mm in diameter, with radial folds on the surface and orange-yellow color (Fig. 1a). The individual bacteria were short, rod-shaped and flagellated (Fig. 1b). Phylogenetic analysis of the strain OX-1 showed a 99% sequence similarity with *Azospirillum brasilense* Gr29 strain (Fig. 1c), suggesting that the strain OX-1 may belong to *Azospirillum* genus. The 16S rRNA gene sequence is available in NCBI GenBank (accession number: OQ152633). Physiological and biochemical characteristics of strain OX-1 are reported in Table 1. The growth curve of strain OX-1 cultured in LB liquid medium at 30 °C and 180 rpm is shown in Figure S1.

Determination of relevant physicochemical indicators during the degradation of calcium oxalate by strain OX-1

Strain OX-1 grew rapidly in a liquid medium with calcium oxalate as the main carbon source and was accompanied by the formation of secondary mineral carbonates. Figure 2 shows the results of the analysis of the relevant physicochemical indicators for the degradation of calcium oxalate by the strain OX-1.

The change in pH within the culture solution during the degradation of calcium oxalate by strain OX-1 is significant (Fig. 2a), but the pH of the uninoculated control group (CK) did not change significantly with duration of incubation and remained about 7.00. The treatment group (T) inoculated with strain OX-1 demonstrated an increase of about 1.3 in the pH of the culture solution to a final value exceeding 8.20, providing a favorable alkaline environment for the formation of carbonate.

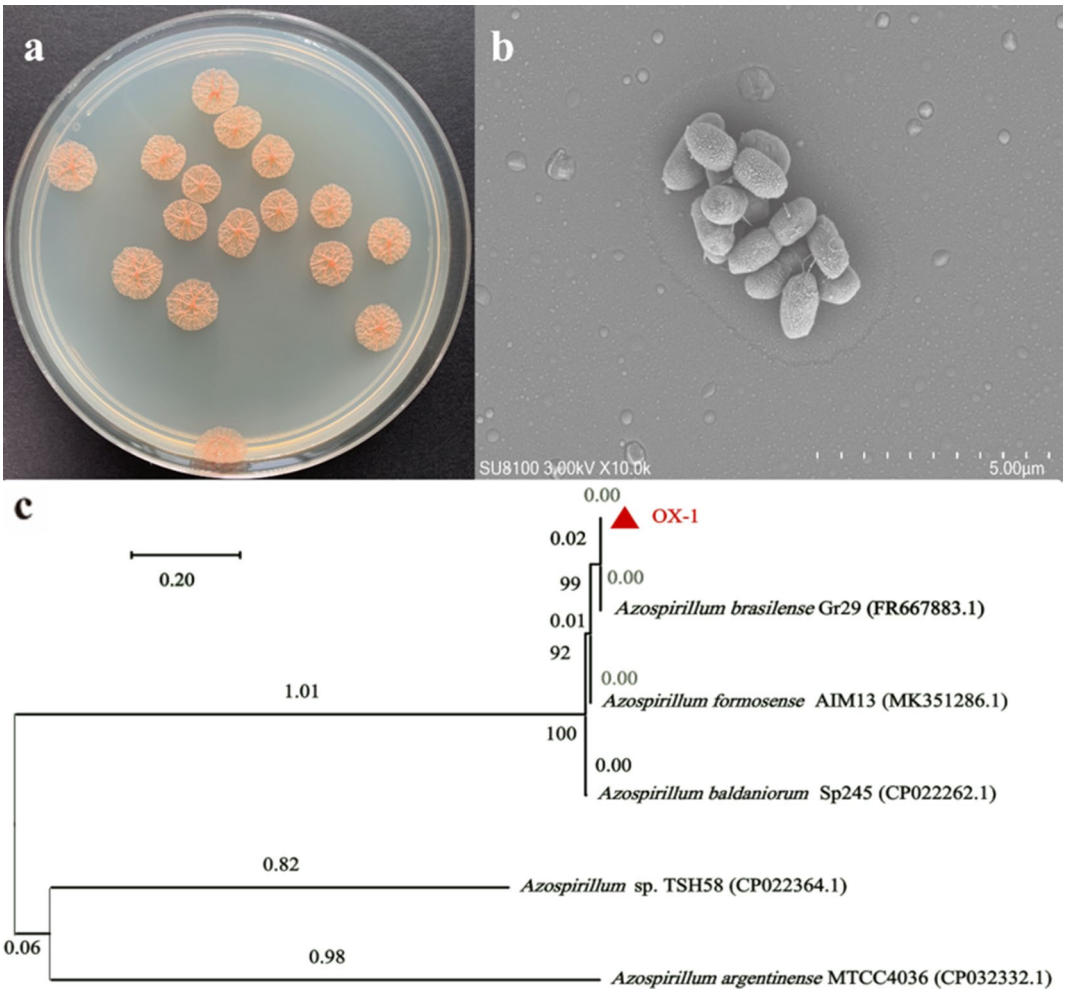

Fig. 1. Morphology and phylogenetic tree of strain OX-1. (**a**) Strain OX-1 was cultured on LB medium at 30 °C for 5 days to form colonies. (**b**) Individual morphology seen under a scanning electron microscope. (**c**) Phylogenetic tree based on 16S analysis showed the phylogenetic relationship between strain OX-1 and related species.

Test	Result	Test	Result
Nitrogen fixation	+	Methyl Red (MR)	-
Cellulase	-	Voges-Proskauer (VP)	-
Amylase	-	Urease	+
Gelatin liquefaction	-	Nitrate reduction	+
Peroxidase	+	H_2S production	-

Table 1. Physiological and biochemical characteristics of strain OX-1. + indicates a positive characteristic; - indicates that the characteristic is negative

The change in $C_2O_4^{2-}$ concentration in the T group during the degradation of calcium oxalate is remarkable compared with the CK group (Fig. 2b). Strain OX-1 is grown in a medium with calcium oxalate as the main carbon source, and first needs to degrade calcium oxalate to form $C_2O_4^{2-}$ and Ca^{2+}, and then transport the $C_2O_4^{2-}$ into the cell to be utilized as a carbon source. The $C_2O_4^{2-}$ concentration in the culture solution was 65 mg/L at day 0, this may be caused by the dissolution of trace amounts of calcium oxalate with the increase in temperature during the sterilization of the medium. The $C_2O_4^{2-}$ concentration in the CK group remained constant throughout the incubation. The $C_2O_4^{2-}$ concentration in the T group decreased rapidly to below 10 mg/L after one day, and thereafter to 0 by 4 days, indicating that bacterial growth led to the degradation of $C_2O_4^{2-}$.

The variations in Ca^{2+} concentration in the culture broth during the degradation of calcium oxalate by strain OX-1 are shown in Fig. 2c. The Ca^{2+} concentration in the T group was highest at day 1, declining continuously to equilibrium at day 5. Apparently, this is because Ca^{2+} is released during the growth of OX-1 as calcium

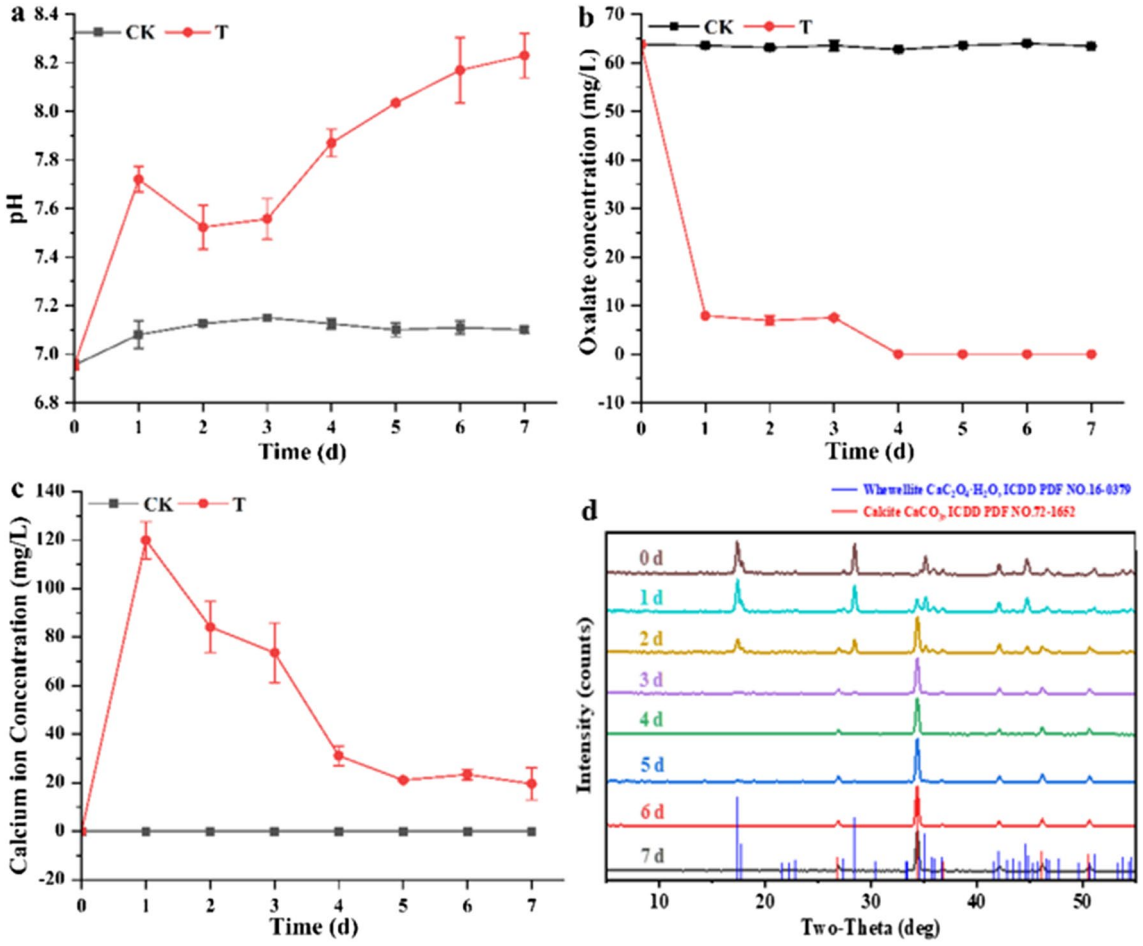

Fig. 2. Analysis of physical and chemical indices related to degradation of calcium oxalate by strain OX-1. (Group CK was treated without strain OX-1; Group T was treated with strain OX-1) (**a**) Changes in pH. (**b**) Changes in oxalate concentration. (**c**) Changes in Ca^{2+} concentration. (**d**) Changes in XRD patterns.

oxalate is degraded and the Ca^{2+} is used during formation of the secondary mineral calcium carbonate, so Ca^{2+} concentration decreases continuously. XRD analysis of the precipitates in the culture solution showed the formation of calcium carbonate crystals (Fig. 2d). With increasing incubation time the characteristic peaks of calcium oxalate (whewellite $CaC_2O_4 \cdot H_2O$, ICDD PDF NO.16–0379) in the inoculated T group gradually became weaker, while the characteristic peaks of calcite type calcium carbonate (calcite $CaCO_3$, ICDD PDF NO.72-1652) increased continuously. By day 3, the characteristic peak of calcium oxalate had disappeared completely and the only crystalline mineral in the precipitate was calcite. In contrast, the Ca^{2+} concentration in the CK group remained constant throughout incubation, and the XRD pattern of the precipitate in the control group also consistently showed calcium oxalate.

These results indicate the strain OX-1 is very efficient at degrading calcium oxalate, and the degradation efficiency even reached 100% by the 3rd day of culture.

Analysis of the main secondary products formed during degradation of calcium oxalate by strain OX-1

Calcite in the precipitate of the T group culture system on the third day was analyzed and the results are shown in Fig. 3.

The presence of certain functional groups can be determined qualitatively by comparing the wavelength positions of specific absorption peaks in the infrared spectrum. The IR spectra of strain OX-1 degradation of calcium oxalate forming calcite (calcium carbonate) are shown in Fig. 3b. For better comparative analysis, the IR spectrum of reagent grade calcium oxalate is also included for reference. The IR spectra reveal characteristic peaks at 2514, 1421, 1082, 871 and 711 cm^{-1} suggesting calcite type calcium carbonate. Among these, the absorption peaks at 871 and 711 cm^{-1} are in-plane or out-of-plane bending vibration peaks of carbonate ions. In addition to the characteristic peaks of calcite, peak patterns of O-H (3422 cm^{-1}), C-H (2980 cm^{-1}, 2930 cm^{-1}), C=O (1800 cm^{-1}) were also detected. These organic functional groups may originate from bacterial cells or from bacterial metabolites.

Thermogravimetric differential thermal analysis (TG-DTA) is used to study the thermal stability and organic matter content of materials. The results of TG-DTA analysis are shown in Fig. 3c and d. The secondary calcite has a significant mass loss in the temperature range of 25–1000 °C, which can be divided into three stages. The

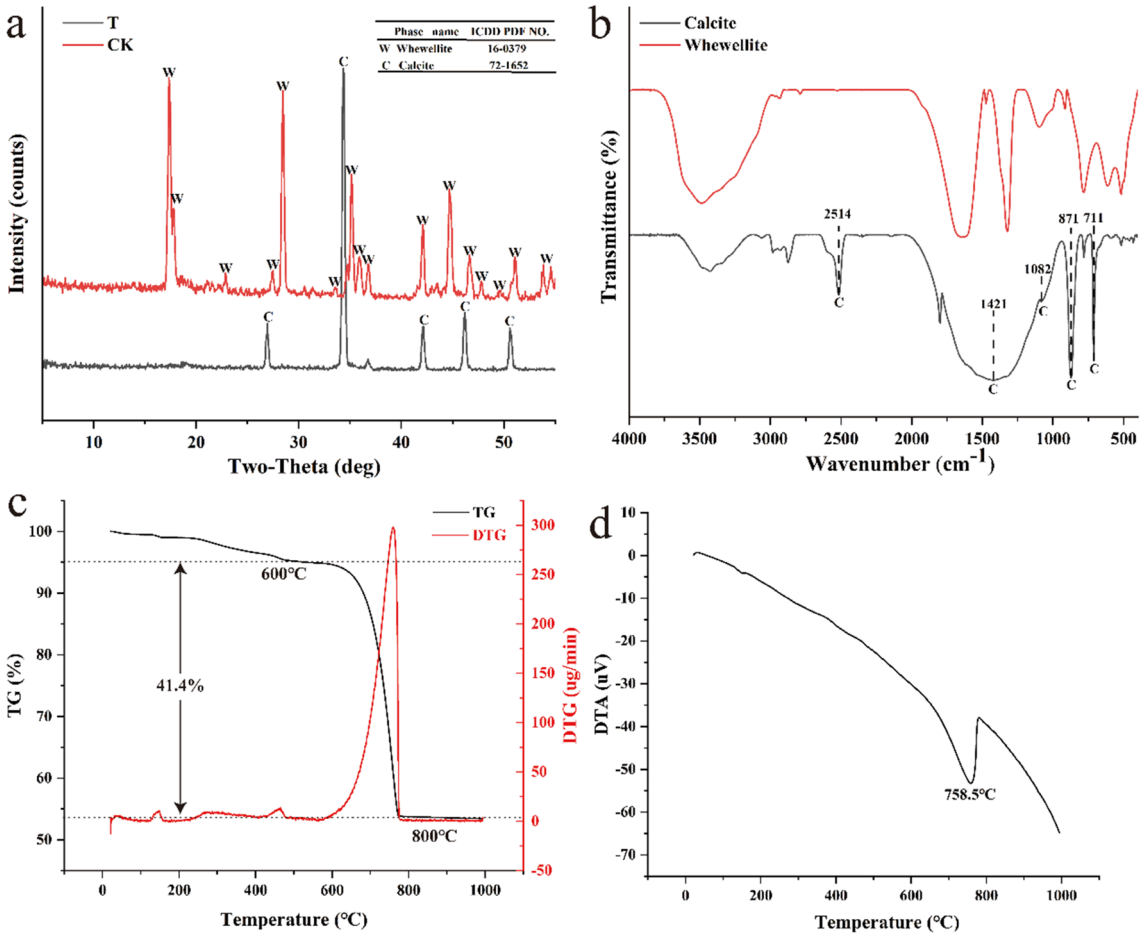

Fig. 3. Analysis of secondary minerals formed by strain OX-1 degradation of calcium oxalate. (**a**) Comparison of XRD patterns. (**b**) Comparison of FTIR spectra of secondary minerals. (**c**) TG-DTG curves of secondary mineral. (**d**) DTA curve of secondary mineral.

fluctuations of the TG and DTG curves show that the first stage mass loss (1.0%) is in the temperature range of 25–200 °C, there is a small heat absorption peak in the DTA curve (Fig. 3d) at 149 °C, which is mainly due to the evaporation of free water from the mineral surface. The mass loss in the second stage (2.9%) was in the temperature range 200–500 °C, and the organic matter content in the culture system was minimal, resulting in only a small change in the TG-DTG curve and an insignificant exothermic peak in the DTA curve. The third stage of mass loss (41.4%) shows a faster mass loss of minerals in the range of 600–800 °C and the DTA curve has a strong heat absorption peak at 758 °C, due to the decomposition of calcite into CaO and CO_2 with increasing temperature. Thereafter the mass of the mineral no longer changes as the temperature increases. The thermal weight loss of calcium carbonate formed in this experiment was about 46.6%. In summary, the results indicated that the strain degraded calcium oxalate to form calcite with only a small amount of organic matter.

The microscopic morphological characteristics of the secondary mineral calcite formed during the degradation of calcium oxalate by the OX-1 strain were further observed and analyzed using Field-Emission Scanning Electron Microscopy (FE-SEM), and the results are shown in Fig. 4. The reagent calcium oxalate is monoclinic prisms (Fig. 4a and b), and its elemental composition is C, O and Ca (Fig. 4c). The morphology of calcite-type calcium carbonate formed after 4 days of weathering by the OX-1 strain (Fig. 4d and e), revealing many lamellar rhombohedral particles aggregated together, and its elemental composition is C, O, and Ca (Fig. 4f). In summary, OX-1 can rapidly degrade calcium oxalate and form a new secondary mineral calcite.

Surprisingly, methane was detected within the culture system of strain OX-1 degrading calcium oxalate (Fig. 5). Compared with the peak area of the CK group, the methane peak area of the T group increased significantly by 80.7% ($P<0.001$).

Differential proteomics analysis and validation of calcium oxalate degradation by strain OX-1

To further investigate the molecular mechanism of calcium oxalate degradation by this strain, a proteomic analysis approach was used. 4D-label-free proteomic analysis was performed on bacterial samples from treatments C and G after 36 h incubation, and a total of 5019 proteins was identified. Using Foldchange ≥ 2.0 or Foldchange $\leq 1/2.0$ and $P<0.05$ as the screening criteria, a total of 875 differential proteins was screened, including 399 up-regulated proteins and 476 down-regulated proteins (Fig. S2). The GO database was used to

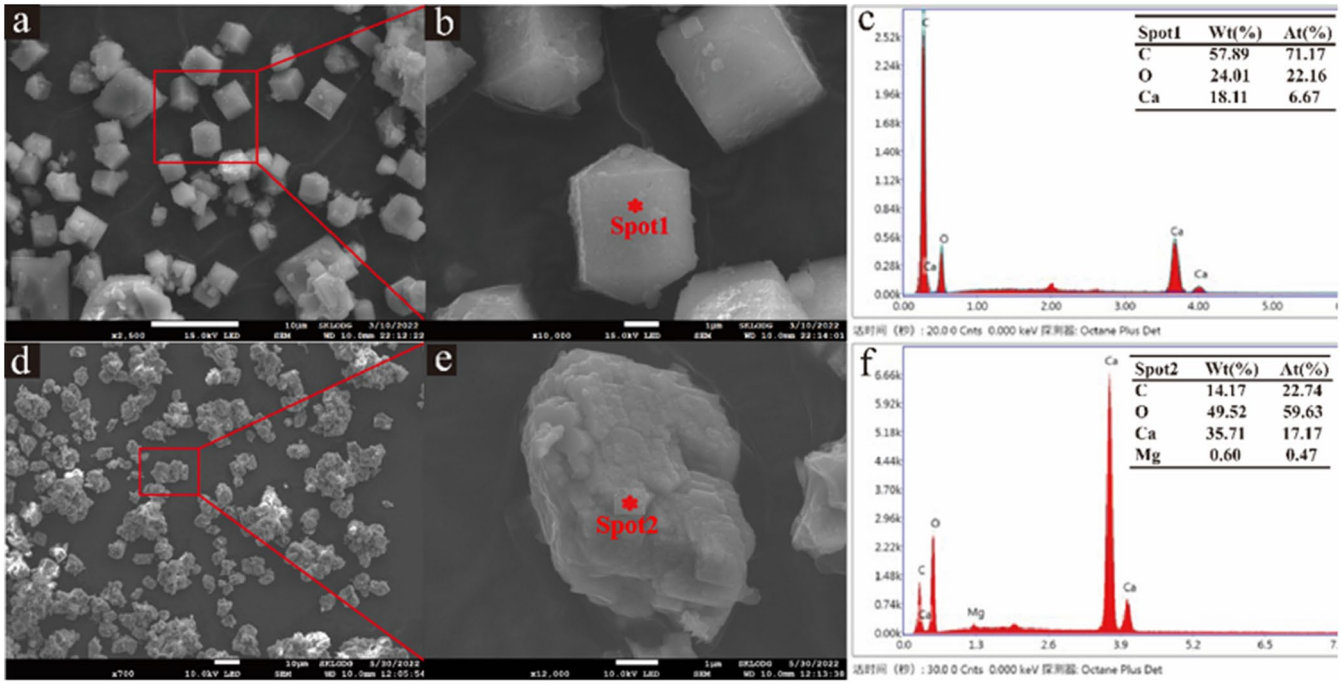

Fig. 4. Morphological observations of secondary minerals of OX-1 degrading calcium oxalate. (**a**-**c**) FE-SEM/EDS results of the reference reagent chemical calcium oxalate. (**d**-**f**) FE-SEM/EDS analysis of secondary minerals formed by strain OX-1 degradation of calcium oxalate for 4 days.

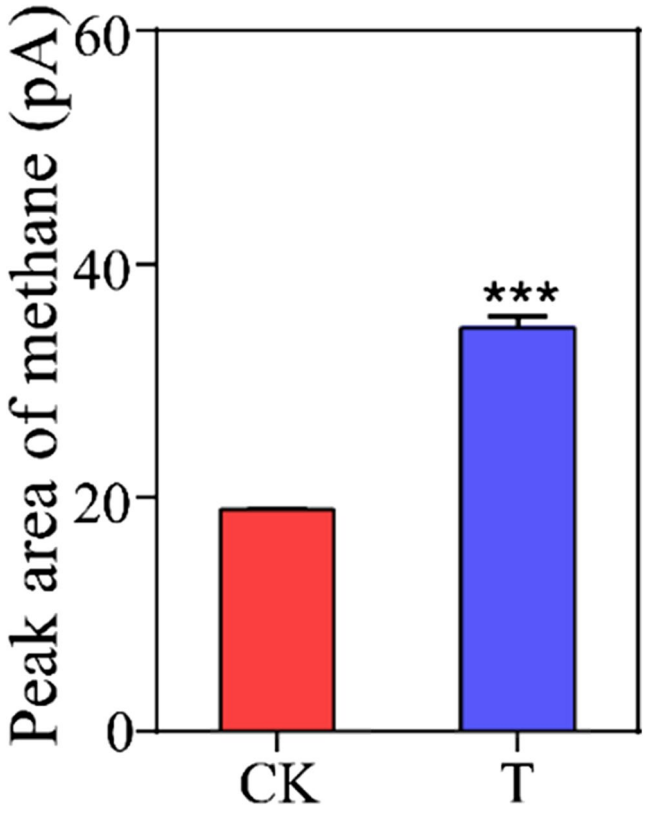

Fig. 5. Peak area of methane. (CK was a blank control without OX-1; T indicates CH_4 content in conical bottle after calcium oxalate was degraded by OX-1.).

annotate the functions of all differentially expressed proteins; the resulting differentially expressed proteins were analyzed using the KEGG database.

Figure 6a depicts the results of GO analysis of the proteins up-regulated in group C vs. group G. The main biological processes (BP) in which the up-regulated differential proteins are involved include oxalate catabolic process, thiamine diphosphate biosynthetic process, and response to oxidative stress. The cellular components (CC) where the up-regulated differential proteins perform their functions are mainly integral components of membranes, cytoplasm and ATP-binding cassette (ABC) transporter complex. The main molecular functions (MF) of the up-regulated differential proteins include metal ion binding, oxidoreductase activity, iron-sulfur cluster binding, isomerase activity, ligase activity, formyl-CoA transferase activity, and oxalate transmembrane transporter activity.

The main biological processes (BP) in which the down-regulated differential proteins (Fig. 6b) are involved include signal transduction, chemotaxis, phosphorelay signal transduction system, bacterial-type flagellum-dependent cell motility and regulation of nitrogen utilization. The cellular components (CC) where the down-regulated differential proteins perform their functions are mainly integral component of membrane and the plasma membrane. The molecular functions (MF) of the down-regulated differential proteins are mainly phosphorelay sensor kinase activity and transmembrane signaling receptor activity.

The differentially up-regulated proteins (Fig. 7a) were mainly enriched in metabolic pathways involving methane metabolism, glyoxylate and dicarboxylate metabolism and thiamine metabolism. The large bubbles and small *P*-values for these metabolic pathways indicate a very high statistical level of significance. The down-

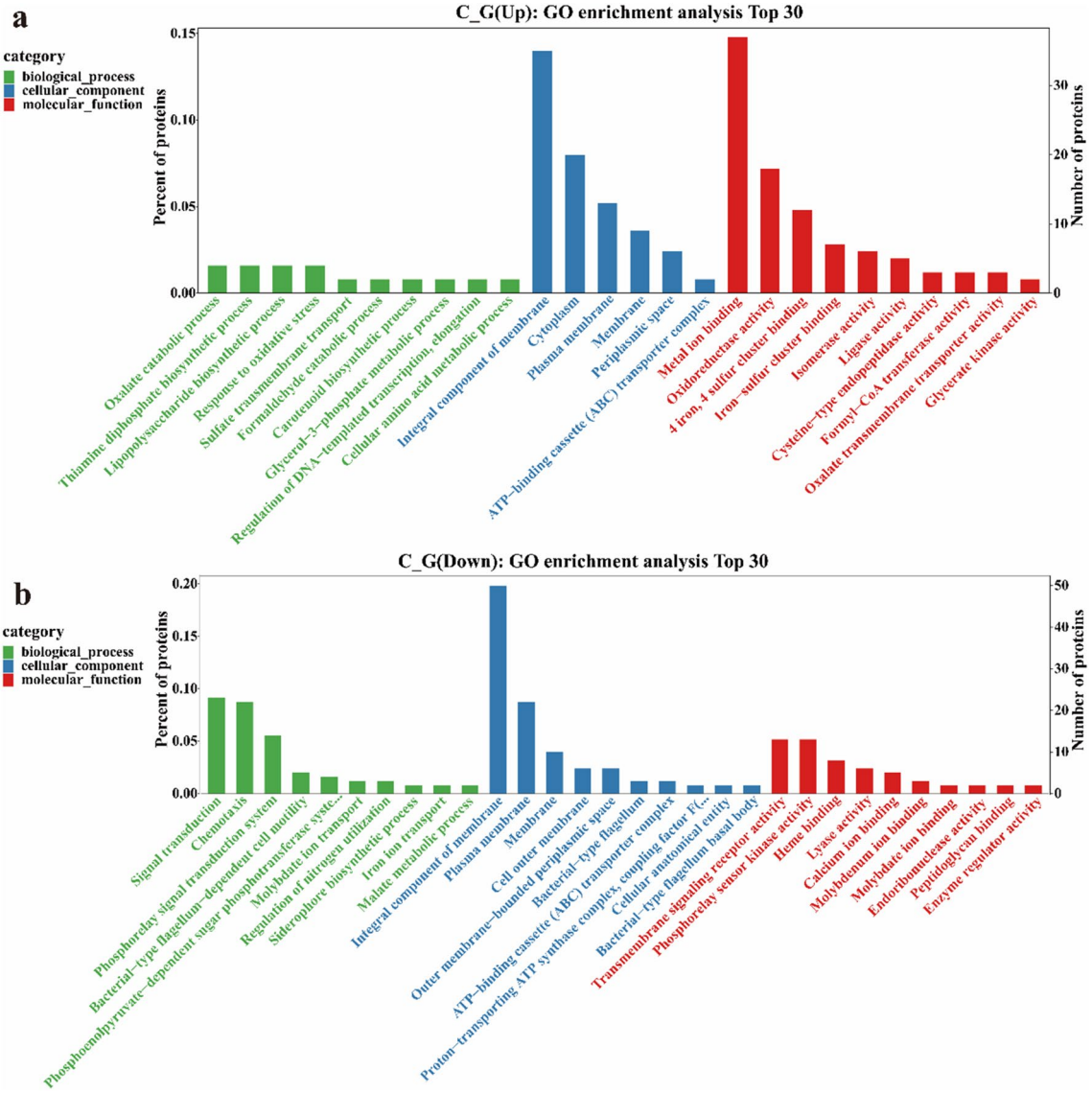

Fig. 6. Top 30 results of differential protein GO enrichment analysis. (**a**) Up-regulation in C vs. G. (**b**) Down-regulation in C vs. G. (C and G refer to treatment groups where the carbon sources are calcium oxalate and glucose, respectively. The same below.).

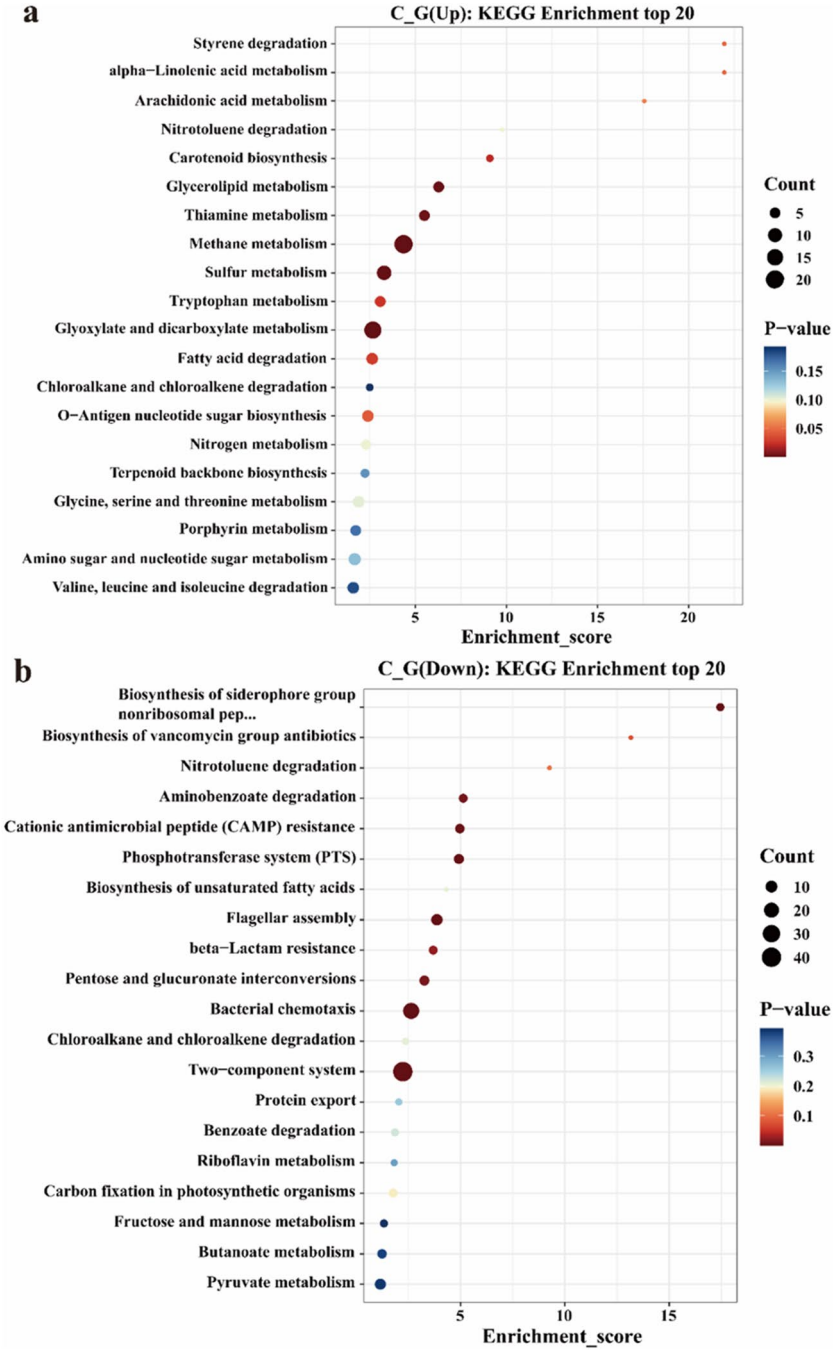

Fig. 7. Top 20 bubble map of KEGG pathway enrichment analysis of differential proteins. The X-axis is the enrichment score, and Y-axis is pathway information of Top20. The entries with larger bubbles contained more differentially regulated proteins, and the color of bubbles changes from blue to red with increasing statistical significance (smaller *P*-value). (**a**) C vs. G up-regulated KEGG enrichment analysis bubble map. (**b**) C vs. G down-regulated KEGG enrichment analysis bubble map.

regulated proteins (Fig. 7b) are mainly enriched in cellular processes such as bacterial chemotaxis, flagellar assembly and two-component system.

Overall, when strain OX-1 was incubated in an environment in which calcium oxalate was the main carbon source, it up-regulated the expression of enzymes to degrade calcium oxalate to obtain organic carbon for growth, and also up-regulated the expression of methane synthesis-related enzymes to synthesize methane.

Discussion

Analysis of the molecular OCP transformation pathway in strain OX-1

The bacterially-mediated OCP pathway in soil has received widespread attention and is considered to be important in generating a potential long-term terrestrial sink for atmospheric CO_2. In this study, an efficient oxalate-degrading bacterium, *Azospirillum* sp. OX-1, was screened (Figs. 1 and 2).

Oxalate metabolism in bacteria involves three key proteins, formyl-CoA transferase, oxalyl-CoA decarboxylase and formate/oxalate reverse transporter (OxlT)[18]. The results of GO enrichment analysis in this study showed that all three key proteins involved in the oxalate metabolic pathway were significantly enriched (Fig. 6, Table S1). KEGG analysis also showed a significant up-regulation of thiamin pyrophosphate anabolism, as a coenzyme of oxalyl-CoA decarboxylase apparently favoring the degradation of calcium oxalate (Fig. 7). In addition, down-regulation of flagellar-associated proteins (Table S1) indicates that strain OX-1 requires focused energy to degrade calcium oxalate and did not require additional motility provided by flagella[37].

The suggested process of calcium oxalate degradation by strain OX-1 is shown in Fig. 8, based on Daniel, et al.[18] and the proteomic analysis in the present study. Bacteria first transport extracellular oxalate ions into the cell using the OxlT transporter protein, activation of oxalic acid to form oxalyl-CoA takes place by addition of CoA molecules under the action of intracellular formyl-CoA transferase. Oxalyl-CoA is then decarboxylated by oxalyl-CoA decarboxylase to produce CO_2 and formate, and CO_2 is released extracellularly. Part of the formate is then converted to formyl-CoA which enters the oxalic acid conversion cycle. The other part is transported outside the cell by OxlT for oxalate transport. Formate: Oxalate reverse transporter (OxlT), which imports oxalate into the cell as a second-order anion and exports formate as a monovalent anion, is thought to generate electrochemical and proton gradients across the cell membrane, which are then used to drive ATP synthesis by ATP synthase[38,39], for use in bacterial growth and metabolism.

Knutson, et al.[40] isolated eight strains of *Streptomyces* from ectomycorrhizal pine roots, all with the ability to degrade oxalate, but did not explore the presence of the OCP pathway in these isolates. It has also been reported that an oxalate-degrading strain of *Oxalobacter formigene* grew with oxalate as the sole carbon and energy source, and that 99% of oxalate was converted to CO_2 and formate[17,41,42], but the coupling of these processes with the synthesis of carbonates was not discussed. Sun, et al.[26] screened an oxalate-degrading strain *Streptomyces* sp. NJ10 which degraded nearly 88% of the supplied calcium oxalate (25 mM/L) after 144 h of incubation and the XRD results showed the formation of a small amount of carbonate 7.6 ± 3.6%. Apparently, strain OX-1, isolated in the present study, was more effective in degrading insoluble oxalate and could degrade all the calcium oxalate within 72 h (Fig. 2). During the high-temperature steam sterilization of the culture medium, an increase in temperature and pressure can enhance the ionization capacity of water, resulting in a greater release of H^+ and OH^-. This phenomenon elevates the solubility of calcium oxalate within the liquid phase, leading to the generation of free $C_2O_4^{2-}$ and Ca^{2+}. However, due to the presence of SO_4^{2-}, CO_3^{2-}, PO_4^{3-} and organic yeast extract in the culture medium, the released Ca^{2+} tend to react with them to precipitate. This procedure resulted in a higher concentration of $C_2O_4^{2-}$ but Ca^{2+} concentration is almost 0 in the supernatant. Oxalyl-CoA decarboxylase catalyzes the decarboxylation of oxalyl-CoA to produce CO_2 and formate, with CO_2 released outside the cell to

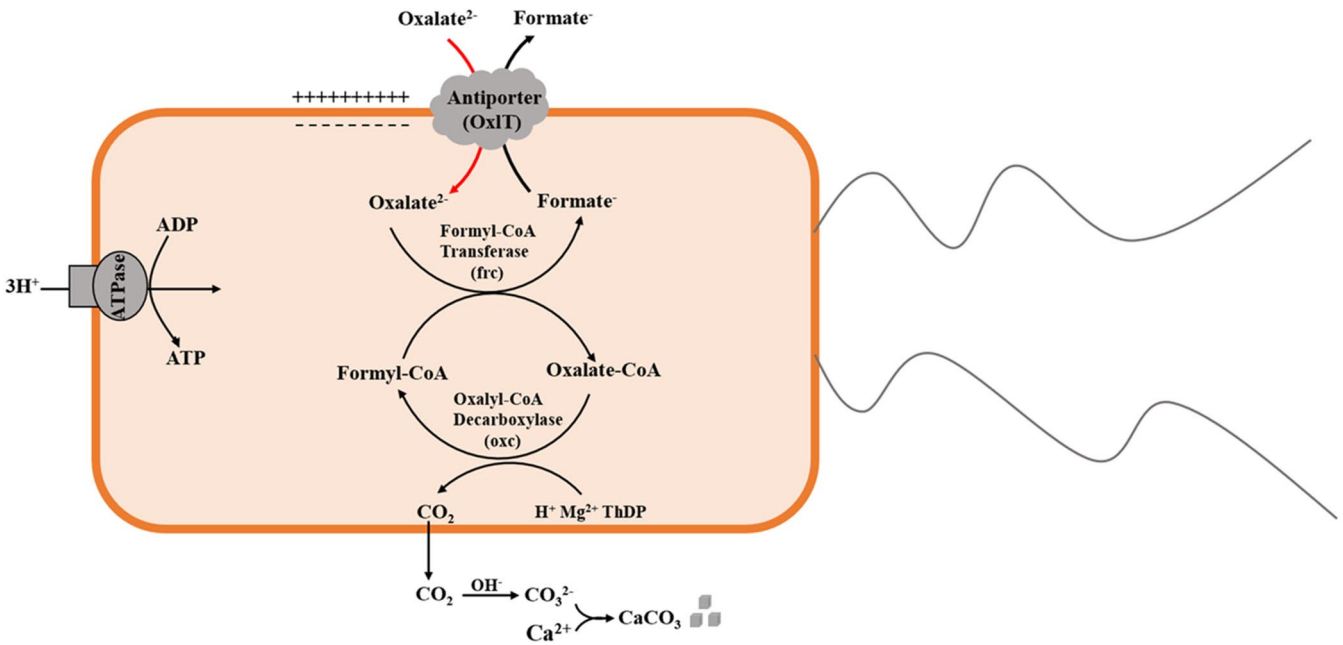

Fig. 8. OCP pathway for calcium carbonate formation by strain OX-1 degrading calcium oxalate, the calcium carbonate formation pathway was added on the basis of Daniel, et al.[18]. (OxlT: formate/oxalate reverse transporter; ThDP: thiamine pyrophosphate).

form carbonate ions by spontaneous hydration under alkaline conditions and combining with Ca^{2+} within the culture medium to form the secondary mineral calcite (Fig. 4).

Additions to the OCP conversion pathway

In this study, gas chromatographic detection results showed that methane content in the culture system was significantly higher than that in the control group at 36 h ($P < 0.001$), and the methane peak area increased by 82% (Fig. 5). Meanwhile, 4d-lab-free proteomic analysis also found significant enrichment and up-regulation of proteins related to methane metabolic pathways (Fig. 7, Table S1). These results all suggest that methane is produced under aerobic conditions during OCP conversion, which is a surprising finding.

According to the oxalate degradation model proposed by Daniel, et al.[18] and the results from this study (Fig. 8), a large amount of formic acid could be produced and transported out of cells during OX-1 degrading calcium oxalate. The high amount of formate in the culture system is a stress factor for the bacterial growth[43], and the bacteria need to remove this intermediate product during the metabolism of oxalate to prevent formate accumulation in the culture system. The increased expression of formate dehydrogenase (Table S1) helps drive the conversion of formic acid. Methanogenic bacteria cause the decomposition of high molecular weight organic matter to produce low molecular weight organic matter during the metabolism. These intermediate products such as hydrogen, small molecules of organic matter and carbon dioxide are ultimately removed by methanogenesis. On the basis of the proteomic results, we speculate that OX-1 may have used both H_2 and CO_2 and methyl compounds as substrates to synthesize methane.

Three types of methanogenic bacteria have been reported, acetotrophic, methylotrophic and hydrogenotrophic, using H_2 & CO_2 as substrates[44]. All three methane synthesis pathways culminate in the formation of methyl coenzyme M, which is catalyzed by methyl coenzyme M reductase I (MCR I) and methyl coenzyme M reductase II (MCR II) with the ultimate formation of methane[45]. Except for some specialized acetotrophic and methylotrophic methanogens, more than 75% of the model strains cultivated so far are hydrogenotrophic methanogens, which use H_2 & CO_2 to produce methane[46]. This is because the hydrogenotropic methanogenic pathway has a higher energy acquisition efficiency than the other two types of methanogenic pathway. In the standard thermodynamic state the reduction of 1 mol CO_2 to methane releases 131 kJ of energy, which is higher than that of methanol to methane (-106 kJ) and acetic acid to methane (-36 kJ)[44,47]. The CO_2 reduction pathway is therefore widely found in nature. In the CO_2 reduction pathway, most methanogenic bacteria are able to reduce CO_2 using formate as an electron donor. They convert four molecules of formate to four of CO_2 and four of H_2 by relying on F420 formate dehydrogenase and F420 reductive hydrogenase, and reuse of H_2 and CO_2 to produce methane[48]. Up-regulated expression of formate dehydrogenase (FDH) catalyzing formate dehydrogenation to form CO_2 and molybdenum nitrogen fixing enzyme (NifO) expression catalyzing the formation of H_2, but no reductive hydrogenase (Table S1), that may provide H_2 and CO_2 for the hydrogenotrophic synthesis of methane. Moreover, the up-regulated expression of enzymes required for the synthesis of methane with H_2 and CO_2 as substrates were also detected (Table S1), suggesting that this pathway for the synthesis of methane may also exist in strain OX-1.

It has also been reported that some species can also use H_2 and CO_2 to synthesize methane except the *Methanosarcinales* family capable of synthesizing methane using methyl-containing compounds such as methanol, ethanol, and methylamine[49]. The proteomic results of the present study revealed up-regulated expression of PQQ-dependent dehydrogenase (Table S1) to reduce formaldehyde to methanol as a feedstock for the synthesis of methane. This suggests that there is a methanogenic pathway in the calcium oxalate culture system that uses H_2 and CO_2 as substrates, as well as a pathway from formate to formaldehyde to methanol and finally methanol as a substrate, to synthesize methane. The postulated reaction processes of methanogenesis by OX-1 using the H_2 reduction CO_2 pathway and methanogenesis using methanol are shown in Fig. 9.

His process requires the participation of several substrates and enzymes, among which FMD, FTR, MCH, MTD and PQQ-dependent dehydrogenase were up-regulated in this experimental proteome (Table S1). However, probably due to the effect of sample collection time and detection error, Methyl coenzyme M reductase (MCR), which is required for the final step of the reaction to synthesize methane, was not detected to be up-regulated, and further research is still required to clarify the mechanism.

Possible reasons for bacterial synthesis of methane include the alleviation of formate stress and the utilization of intermediates in the process of methane synthesis. The KEGG map of the present study showed that H_4MPT, an intermediate product of methane metabolism (azt00680), could be involved in folate biosynthesis (azt00790). Folate is an important substance involved in nucleic acid synthesis and cell division and differentiation[50,51], and is essential for bacterial survival.

Anti-oxidant protection mechanism during methane synthesis

The formation of methane in the present study contradicts the previously reported details of the OCP pathway and the accepted idea that methanogenic bacteria produce methane mainly under anaerobic conditions. In fact, as early as 1991, Kiene et al. discovered the phenomenon of methane supersaturation in the upper layers of the ocean, and proposed the oceanic methane paradox[52,53]. Methane production by eukaryotes in terrestrial ecosystems under aerobic conditions has been reported[54], microbial use of methylation metabolites from phytoplankton to produce methane in oxygenated seawater has also been reported[55–59] and these findings suggest that methanogenesis goes beyond the boundary of hypoxia in the traditional sense.

The molecule mechanism of methane production by microorganisms in the presence of oxygen is not clear. There are two main possibilities that have been reported: one is that microorganisms can counteract the effect of molecular oxygen during methanogenesis by the action of corresponding enzymes in an oxygenated environment, or there is some mechanism for the microorganism to counteract the effects of oxygen, such as achieving an anaerobic state inside the cell through respiration[58]. The other possibility is that they use

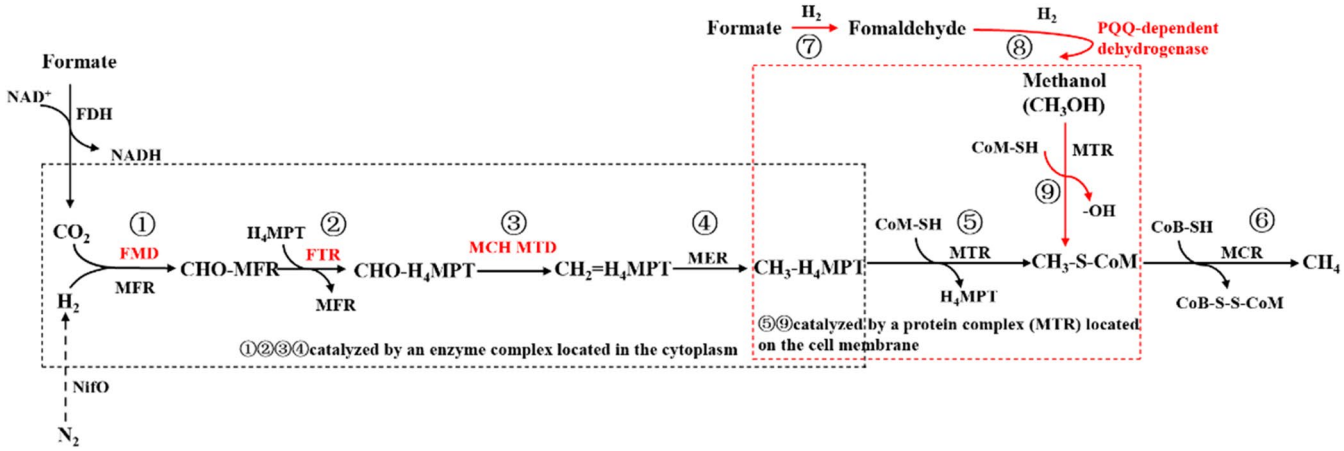

Fig. 9. Diagram of the postulated methane production process in strain OX-1 with $H_2$and CO_2(①②③④⑤⑥) and methanol (⑦⑧⑨⑥) as substrates. (catalyzed by enzyme complexes located in the cytoplasm ①②③④; and protein complexes located on the cell membrane ⑤⑨) (MFR, methanofuran; H_4MPT, tetrahydromethanopterin; CoM-SH, Coenzyme M; CoB-SH, Coenzyme B; CoM-S-S-CoB, heterodisulfide; FMD, formyl-methanofuran dehydrogenase; FTR, formyl-methanofuran-H_4MPT formyltransferase; MCH, methyl-H_4MPT cyclohydrolase; MTD, methylene-H_4MPT dehydrogenase; MER, methylene-H_4MPT reductase; MTR, methyl-H_4MPT-CoM-methyltransferase; MCR, methyl-Coenzyme M reductase; NifO, molybdenum azotozyme; FDH, formate dehydrogenase.).

biochemical pathways that do not involve oxygen-sensitive enzymes like those in conventional pathways, for example, methane production using alternative pathways that do not involve oxygen-sensitive enzymes[60]. For example, the enzyme encoded by the *phnJ* gene, is insensitive to oxygen and can therefore produce methane under aerobic conditions[60]. However, the enzyme encoded by this gene was not significantly up-regulated or down-regulated by differential expression in the proteomic analysis in the present study.

The strain OX-1 is most likely to counteract the effect of molecular oxygen during methane synthesis through the relevant enzymes. It has been reported that many oxygen-tolerant microorganisms have peroxidases encoded by a single gene in the antioxidant enzyme system[61,62]. For example, desert soil methanogenic bacteria actively transcribe oxygen detoxification genes to express hydrogen peroxidase[63]. In this study, proteins associated with oxidative stress processes were significantly enriched and upregulated expression of catalase, organic hydrogen peroxide resistance protein and glutathione peroxidase (Fig. 6, Table S1). So it may be that the expression of these enzymes counteracts the negative effects of oxygen, thus creating the conditions for methane synthesis. This study suggests that methane production can occur when methanogenic archaea and anaerobic conditions are absent.

The PRM validation results (Fig. S3) were highly consistent with the 4D-label free proteomics results, indicating that the 4D-label free proteomics analysis was correct.

Conclusions

In this study, an efficient oxalate-degrading strain designated *Azospirillum* sp. OX-1 was isolated. The changes in the differential proteome during degradation of calcium oxalate by this bacterium were investigated, and the proteins formyl-CoA transferase, oxalyl-CoA decarboxylase, and formate/oxalate reverse transporter, which are related to calcium oxalate degradation, were all found to be enriched. This molecular evidence helps to resolve the mechanism of oxalate biodegradation coupled with carbonate synthesis. More importantly, the accompanying production of methane, and enrichment of proteins related to the methane metabolic pathway revealed by the present study, are of environmental significance when considering the role of the OCP in sequestration of atmospheric CO_2. The degradation of oxalate to carbonate has previously been regarded as an important potential mechanism in the sequestration of atmospheric CO_2 to mitigate climate change, but methane also has serious negative effects on the global climate. It is therefore an important future research priority to examine how widespread the methanogenic activity demonstrated in the present study is in different environments and other bacterial strains and species.

Data availability

The datasets used and/or analysed during the current study will be available from the corresponding author on reasonable request.

Received: 10 April 2024; Accepted: 30 September 2024
Published online: 09 October 2024

References

1. Arvieu, J. C., Leprince, F. & Plassard, C. Release of oxalate and protons by ectomycorrhizal fungi in response to P-deficiency and calcium carbonate in nutrient solution. *Ann. For. Sci.* **60**, 815–821. https://doi.org/10.1051/forest:2003076 (2003).
2. Casarin, V., Plassard, C., Souche, G. & Arvieu, J. C. Quantification of oxalate ions and protons released by ectomycorrhizal fungi in rhizosphere soil. *Agronomie*. **23**, 461–469. https://doi.org/10.1051/agro:2003020 (2003).
3. Van Hees, P. A. W. et al. Oxalate and ferricrocin exudation by the extramatrical mycelium of an ectomycorrhizal fungus in symbiosis with *Pinus sylvestris*. *New Phytol.* **169**, 367–378. https://doi.org/10.1111/j.1469-8137.2005.01600.x (2005).
4. Frey, B. et al. Weathering-associated bacteria from the Damma Glacier forefield: physiological capabilities and impact on Granite Dissolution. *Appl. Environ. Microb.* **76**, 4788–4796. https://doi.org/10.1128/Aem.00657-10 (2010).
5. Stephens, W. E. Whewellite and its key role in living systems. *Geol. Today*. **28**, 180–185. https://doi.org/10.1111/j.1365-2451.2012.00849.x (2012).
6. Sazanova, K. V. et al. Carbonate and oxalate crystallization effected by the metabolism of Fungi and Bacteria in various trophic conditions: the case of Penicillium Chrysogenum and Penicillium chrysogenum with Bacillus subtilis. *Crystals*. **13**, 94. https://doi.org/10.3390/cryst13010094 (2023).
7. Strobel, B. W. Influence of vegetation on low-molecular-weight carboxylic acids in soil solution - a review. *Geoderma*. **99**, 169–198. https://doi.org/10.1016/S0016-7061(00)00102-6 (2001).
8. Smith, R. L. & Oremland, R. S. Anaerobic oxalate degradation: widespread natural occurrence in aquatic sediments. *Appl. Environ. Microb.* **46**, 106–113. https://doi.org/10.1128/aem.46.1.106-113.1983 (1983).
9. Miller, A. & Dearing, D. The metabolic and ecological interactions of oxalate-degrading Bacteria in the mammalian gut. *Pathogens*. **2**, 636–652. https://doi.org/10.3390/pathogens2040636 (2013).
10. Hervé, V., Junier, T., Bindschedler, S., Verrecchia, E. & Junier, P. Diversity and ecology of oxalotrophic bacteria. *World J. Microb. Biot.* **32**, 28. https://doi.org/10.1007/s11274-015-1982-3 (2016).
11. Guggiari, M. et al. Experimental calcium-oxalate crystal production and dissolution by selected wood-rot fungi. *Int. Biodeter Biodegr*. **65**, 803–809. https://doi.org/10.1016/j.ibiod.2011.02.012 (2011).
12. Sahin, N. Oxalotrophic bacteria. *Res. Microbiol.* **154**, 399–407. https://doi.org/10.1016/S0923-2508(03)00112-8 (2003).
13. Bravo, D., Braissant, O., Cailleau, G., Verrecchia, E. & Junier, P. Isolation and characterization of oxalotrophic bacteria from tropical soils. *Arch. Microbiol.* **197**, 65–77. https://doi.org/10.1007/s00203-014-1055-2 (2015).
14. Bravo, D. et al. Identification of active oxalotrophic bacteria by bromodeoxyuridine DNA labeling in a microcosm soil experiments. *Fems Microbiol. Lett.* **348**, 103–111. https://doi.org/10.1111/1574-6968.12244 (2013).
15. Daniel, S. L., Pilsl, C. & Drake, H. L. Anaerobic oxalate consumption by microorganisms in forest soils. *Res. Microbiol.* **158**, 303–309. https://doi.org/10.1016/j.resmic.2006.12.010 (2007).
16. Sahin, N., Gonzalez, J. M., Iizuka, T. & Hill, J. E. Characterization of two aerobic ultramicrobacteria isolated from urban soil and a description of *Oxalicibacterium solurbis* sp. nov. *Fems Microbiol. Lett.* **307**, 25–29. https://doi.org/10.1111/j.1574-6968.2010.01954.x (2010).
17. Allison, M. J., Dawson, K. A., Mayberry, W. R. & Foss, J. G. *Oxalobacter formigenes* gen. nov., sp. nov.: oxalate-degrading anaerobes that inhabit the gastrointestinal tract. *Arch. Microbiol.* **141**, 1–7. https://doi.org/10.1007/bf00446731 (1985).
18. Daniel, S. L. et al. Forty years of a gutsy oxalate-degrading specialist. *Appl. Environ. Microb.* **87**, e0054421. https://doi.org/10.1128/AEM.00544-21 (2021).
19. Al, K. F. et al. Oxalate-Degrading mitigates Urolithiasis in a model. *Msphere*. **5**, e00498–e00420. https://doi.org/10.1128/mSphere.00498-20 (2020).
20. Kost, T., Stopnisek, N., Agnoli, K., Eberl, L. & Weisskopf, L. Oxalotrophy, a widespread trait of plant-associated Burkholderia species, is involved in successful root colonization of lupin and maize by *Burkholderia phytofirmans*. *Front. Microbiol.* **4**, 421. https://doi.org/10.3389/fmicb.2013.00421 (2014).
21. Miller, A. W., Kohl, K. D. & Dearing, M. D. The gastrointestinal tract of the White-Throated Woodrat (Neotoma albigula) harbors distinct consortia of oxalate-degrading Bacteria. *Appl. Environ. Microb.* **80**, 1595–1601. https://doi.org/10.1128/Aem.03742-13 (2014).
22. Dumas, B., Freyssinet, G. & Pallett, K. E. Tissue-specific expression of Germin-Like Oxalate oxidase during development and fungal infection of Barley Seedlings. *Plant Physiol.* **107**, 1091–1096. https://doi.org/10.1104/pp.107.4.1091 (1995).
23. Lane, B. G. et al. Germin isoforms are discrete temporal markers of wheat development. *Eur. J. Biochem.* **209**, 961–969. https://doi.org/10.1111/j.1432-1033.1992.tb17369.x (2005).
24. Svedruzic, D. et al. The enzymes of oxalate metabolism: unexpected structures and mechanisms. *Arch. Biochem. Biophys.* **433**, 176–192. https://doi.org/10.1016/j.abb.2004.08.032 (2005).
25. Khammar, N. et al. Use of the gene as a molecular marker to characterize oxalate-oxidizing bacterial abundance and diversity structure in soil. *J. Microbiol. Meth.* **76**, 120–127. https://doi.org/10.1016/j.mimet.2008.09.020 (2009).
26. Sun, Q. B., Li, J., Finlay, R. D. & Lian, B. Oxalotrophic bacterial assemblages in the ectomycorrhizosphere of forest trees and their effects on oxalate degradation and carbon fixation potential. *Chem. Geol.* **514**, 54–64. https://doi.org/10.1016/j.chemgeo.2019.03.023 (2019).
27. Syed, S., Buddolla, V. & Lian, B. Oxalate Carbonate Pathway-Conversion and fixation of Soil Carbon-A potential scenario for sustainability. *Front. Plant. Sci.* **11**, 591297. https://doi.org/10.3389/fpls.2020.591297 (2020).
28. Michael, G. et al. Oxalate production by fungi: significance in geomycology, biodeterioration and bioremediation. *Fungal Biol. Rev.* **28**, 36–55. https://doi.org/10.1016/j.fbr.2014.05.001 (2014).
29. Braissant, O., Cailleau, G., Aragno, M. & Verrecchia, E. P. Biologically induced mineralization in the tree (Moraceae): its causes and consequences to the environment. *Geobiology*. **2**, 59–66. https://doi.org/10.1111/j.1472-4677.2004.00019.x (2004).
30. Cailleau, G., Braissant, O., Dupraz, C., Aragno, M. & Verrecchia, E. P. Biologically induced accumulations of $CaCO_3$ in orthox soils of Biga, Ivory Coast. *Catena*. **59**, 1–17. https://doi.org/10.1016/j.catena.2004.06.002 (2005).
31. Rowley, M. C. et al. Moving carbon between spheres, the potential oxalate-carbonate pathway of Sw.; Moraceae. *Plant. Soil.* **412**, 465–479. https://doi.org/10.1007/s11104-016-3135-3 (2017).
32. Nicolas, D., Curtis, H. & Matthew, G. M.Eurasian Soil Sci., C. in *Interpretation of Micromorphological Features of Soils and Regoliths* Vol. 44 (ed Kooistra Maja J.) Ch. 9, 149–194. https://doi.org/10.1016/b978-0-444-53156-8.00009-x (2010)
33. Cailleau, G., Braissant, O. & Verrecchia, E. P. Turning sunlight into stone: the oxalate-carbonate pathway in a tropical tree ecosystem. *Biogeosciences*. **8**, 1755–1767. https://doi.org/10.5194/bg-8-1755-2011 (2011).
34. Cailleau, G., Mota, M., Bindschedler, S., Junier, P. & Verrecchia, E. P. Detection of active oxalate-carbonate pathway ecosystems in the Amazon Basin: global implications of a natural potential C sink. *Catena*. **116**, 132–141. https://doi.org/10.1016/j.catena.2013.12.017 (2014).
35. Jin, Z. X., Wang, C., Dong, W. & Li, X. Isolation and some properties of newly isolated oxalate-degrading *Pandoraea* sp. OXJ-11 from soil. *J. Appl. Microbiol.* **103**, 1066–1073. https://doi.org/10.1111/j.1365-2672.2007.03363.x (2007).
36. Krieg, N. R. *et al. Bergey's Manual® of Systematic Bacteriology*. Vol. 38 443–491. https://doi.org/10.1007/978-0-387-68572-4 (Spring, 2010).
37. Nakamura, S. & Minamino, T. Flagella-Driven motility of Bacteria. *Biomolecules*. **9**, 279. https://doi.org/10.3390/biom9070279 (2019).
38. Anantharam, V., Allison, M. J. & Maloney, P. C. Oxalate:formate exchange. *J. Biol. Chem.* **264**, 7244–7250. https://doi.org/10.1016/s0021-9258(18)83227-6 (1989).

39. Kuhner, C. H., Hartman, P. A. & Allison, M. J. Generation of a proton motive force by the anaerobic oxalate-degrading bacterium *Oxalobacter formigenes*. *Appl. Environ. Microb.* **62**, 2494–2500. https://doi.org/10.1128/aem.62.7.2494-2500.1996 (1996).
40. Knutson, D. M., Hutchins, A. S. & Cromack, K. The association of calcium oxalate-utilizing Streptomyces with conifer ectomycorrhizae. *Antonie Van Leeuwenhoek*. **46**, 611–619 (1980).
41. Dawson, K. A., Allison, M. J. & Hartman, P. A. Isolation and some characteristics of anaerobic oxalate-degrading bacteria from the rumen. *Appl. Environ. Microb.* **40**, 833–839. https://doi.org/10.1128/aem.40.4.833-839.1980 (1980).
42. Cornick, N. A. & Allison, M. J. Assimilation of oxalate, acetate, and CO_2 by *Oxalobacter formigenes*. *Can. J. Microbiol.* **42**, 1081–1086. https://doi.org/10.1139/m96-138 (1996).
43. Laughrea, M. Transfer ribonucleic acid-dependent but ribosome-independent leucine incorporation into rat brain protein. *Biochemistry*. **21**, 5694–5700. https://doi.org/10.1021/bi00265a047 (2002).
44. Ferry, J. G. Methane from acetate. *J. Bacteriol.* **174**, 5489–5495. https://doi.org/10.1128/jb.174.17.5489-5495.1992 (1992).
45. Lai, Z., Huang, G. & Bai, L. Advances of structure, function, and catalytic mechanism of methyl-coenzyme M reductase. *Chin. J. Biotech.* **37**, 4147–4157. https://doi.org/10.13345/j.cjb.200830 (2021).
46. Williams, W. J. & Nash, E. A. A voltage controlled variable frequency generator for neurophysiology. *Med. Biol. Eng.* **6**, 683–685. https://doi.org/10.1007/bf02474733 (1968).
47. Welte, C. & Deppenmeier, U. Bioenergetics and anaerobic respiratory chains of aceticlastic methanogens. *Biochim. Biophys. Acta*. **1837**, 1130–1147. https://doi.org/10.1016/j.bbabio.2013.12.002 (2014).
48. Wood, G. E., Haydock, A. K. & Leigh, J. A. Function and regulation of the formate dehydrogenase genes of the methanogenic Archaeon. *J. Bacteriol.* **185**, 2548–2554. https://doi.org/10.1128/Jb.185.8.2548-2554.2003 (2003).
49. Fang, X., Li, J., Rui, J. & Li, X. Research progress in biochemical pathways of methanogenesis. *Chin. J. Appl. Environ. Biol.* **21**, 1–9. https://doi.org/10.3724/SP.J.1145.2014.08019 (2015).
50. Brown, G. M. The biosynthesis of folic acid. *J. Biol. Chem.* **237**, 536–540. https://doi.org/10.1016/s0021-9258(18)93957-8 (1962).
51. Maekawa, A., Nakajima, H. & Kawata, T. Folic acid. *Nihon Rinsho*. **57**, 2254–2260. https://doi.org/10.1016/0002-9343(46)90039-3 (1999).
52. Gucinski, H. Microbial production and consumption of greenhouse gases: methane, nitrogen oxides, and halomethanes. *J. Environ. Qua*. **23**. https://doi.org/10.2134/jeq1994.00472425002300010034x (1994).
53. Kiene, R. A.S.M., in *Microbial Production and Consumption of Greenhouse Gases: Methane, Nitrogen Oxides and Halomethanes* (eds J. E. Rogers & W. B. Whitman) 111–146. https://doi.org/10.2134/jeq1994.00472425002300010034x (1991).
54. Keppler, F., Hamilton, J. T. G., Brass, M. & Röckmann, T. Methane emissions from terrestrial plants under aerobic conditions. *Nature*. **439**, 187–191. https://doi.org/10.1038/nature04420 (2006).
55. Karl, D. M. et al. Aerobic production of methane in the sea. *Nat. Geosci.* **1**, 473–478. https://doi.org/10.1038/ngeo234 (2008).
56. del Valle, D. A. & Karl, D. M. Aerobic production of methane from dissolved water-column methylphosphonate and sinking particles in the North Pacific Subtropical Gyre. *Aquat. Microb. Ecol.* **73**, 93–105. https://doi.org/10.3354/ame01714 (2014).
57. Damm, E. et al. Methane production in aerobic oligotrophic surface water in the central Arctic Ocean. *Biogeosciences*. **7**, 1099–1108. https://doi.org/10.5194/bg-7-1099-2010 (2010).
58. Damm, E., Rudels, B., Schauer, U., Mau, S. & Dieckmann, G. Methane excess in Arctic surface water- triggered by sea ice formation and melting. *Sci. Rep.* **5**, 16179. https://doi.org/10.1038/srep16179 (2015).
59. Damm, E., Thoms, S., Beszczynska-Möller, A., Nöthig, E. M. & Kattner, G. Methane excess production in oxygen-rich polar water and a model of cellular conditions for this paradox. *Polar Sci.* **9**, 327–334. https://doi.org/10.1016/j.polar.2015.05.001 (2015).
60. Tang, K. W., McGinnis, D. F., Ionescu, D. & Grossart, H. P. Methane production in Oxic Lake Waters potentially increases aquatic methane flux to Air. *Environ. Sci. Tech. Let*. **3**, 227–233. https://doi.org/10.1021/acs.estlett.6b00150 (2016).
61. Haas, A., Brehm, K., Kreft, J. & Goebel, W. Cloning, characterization, and expression in *Escherichia coli.* of a gene encoding Listeria seeligeri catalase, a bacterial enzyme highly homologous to mammalian catalases. *J. Bacteriol.* **173**, 5159–5167. https://doi.org/10.1128/jb.173.16.5159-5167.1991 (1991).
62. Brunder, W., Schmidt, H. & Karch, H. KatP, a novel catalase-peroxidase encoded by the large plasmid of enterohaemorrhagic *Escherichia coli.* O157:H7. *Microbiology*. **142**, 3305–3315. https://doi.org/10.1099/13500872-142-11-3305 (1996).
63. Angel, R., Matthies, D. & Conrad, R. Activation of methanogenesis in arid biological soil crusts despite the oresence of oxygen. *PloS ONE*. **6**, e20453. https://doi.org/10.1371/journal.pone.0020453 (2011).

Acknowledgements

This work was jointly supported by the National Natural Science Foundation of China (Grant Number 92351302; 41772360).

Author contributions

Dening Xia: Methodology, Investigation, Experiment, Data Analysis, Writing – original draft. Wenjun Nie: Methodology, Investigation, Writing – original draft. Xiaofang Li: Experiment, Data Analysis. Roger D. Finlay: Writing – review & discussion. Bin Lian: Conceptualization, Supervision, Project administration, Investigation, Writing – review & editing.

Declarations

Competing interests

The authors declare no competing interests.

Additional information

Supplementary Information The online version contains supplementary material available at https://doi.org/10.1038/s41598-024-74939-8.

Correspondence and requests for materials should be addressed to B.L.